

Cannabinoid overrides triggers of GABAergic plasticity in vestibular circuits and distorts the development of navigation

Highlights

- Early cannabis exposure impairs graviceptive reflexes via presynaptic CB1R
- CB1R activity in early postnatal stages shapes vestibular GABAergic plasticity
- Disinhibitory and inhibitory sites use distinct triggers for eCB-mediated plasticity
- ECB-mediated LTD_{GABA} alters the development of navigation

Authors

Wei Shi, Kenneth Lap-Kei Wu, Mengliu Yang, ..., Chun-Wai Ma, Daisy Kwok-Yan Shum, Ying-Shing Chan

Correspondence

shumdkhk@hku.hk (D.K.-Y.S.), yschan@hku.hk (Y.-S.C.)

In brief

Natural sciences; Biological sciences; Neuroscience



Article

Cannabinoid overrides triggers of GABAergic plasticity in vestibular circuits and distorts the development of navigation

Wei Shi,^{1,4,6} Kenneth Lap-Kei Wu,^{1,3,5,6} Mengliu Yang,^{4,6} Francisco Paulo De Nogueira Botelho,¹ Oscar Wing-Ho Chua,¹ Hui-Jing Hu,¹ Ka-Pak Ng,¹ Ulysses Tsz-Fung Lam,¹ Kin-Wai Tam,^{1,3} Chun-Wai Ma,¹ Daisy Kwok-Yan Shum,^{1,2,3,*} and Ying-Shing Chan^{1,2,3,7,*}

¹School of Biomedical Sciences, Li Ka Shing Faculty of Medicine, The University of Hong Kong, Pokfulam, Hong Kong SAR, P.R. China

²State Key Laboratory of Brain and Cognitive Sciences, The University of Hong Kong, Pokfulam, Hong Kong SAR, P.R. China

³Neuroscience Research Centre, The University of Hong Kong, Pokfulam, Hong Kong SAR, P.R. China

⁴Beijing Advanced Innovation Center for Big Data-based Precision Medicine, School of Engineering and Medicine, Beihang University, Beijing, P.R. China

⁵Present address: Kenneth Wu, MRC Laboratory of Molecular Biology, Cambridge, UK

⁶These authors contributed equally

⁷Lead contact

*Correspondence: shumdkhk@hku.hk (D.K.-Y.S.), yschan@hku.hk (Y.-S.C.)

<https://doi.org/10.1016/j.isci.2025.112566>

SUMMARY

Early life exposure to cannabis can result in long-lasting deficits in spatial navigation. We ask if the development of this behavior is subject to early life activity of type I cannabinoid receptor (CB1R) in the vestibular nucleus. In rodents, we found that local exposure to CB1R agonist within the first postnatal week, but not thereafter, led to a decline in the induction efficacy of long-term depression at GABAergic synapses (LTD_{GABA}), a key step in the hard-wiring of vestibular circuits. Within this critical period, endocannabinoid-mediated LTD_{GABA} at inhibitory neurons was selectively triggered by cholecystokinin, whereas that at excitatory neurons was by serotonin. Neonatal exposure to cannabinoids extended the phase of high GABAergic synaptic plasticity and overrode the synapse-specific, modulatory mechanism for plasticity. Such treatment delayed the postnatal emergence of vestibular-dependent reflexes and deranged adult navigational behavior. Deficits in higher functions are thus attributable to the maldevelopment of sensory processing circuits resulting from early cannabis exposure.

INTRODUCTION

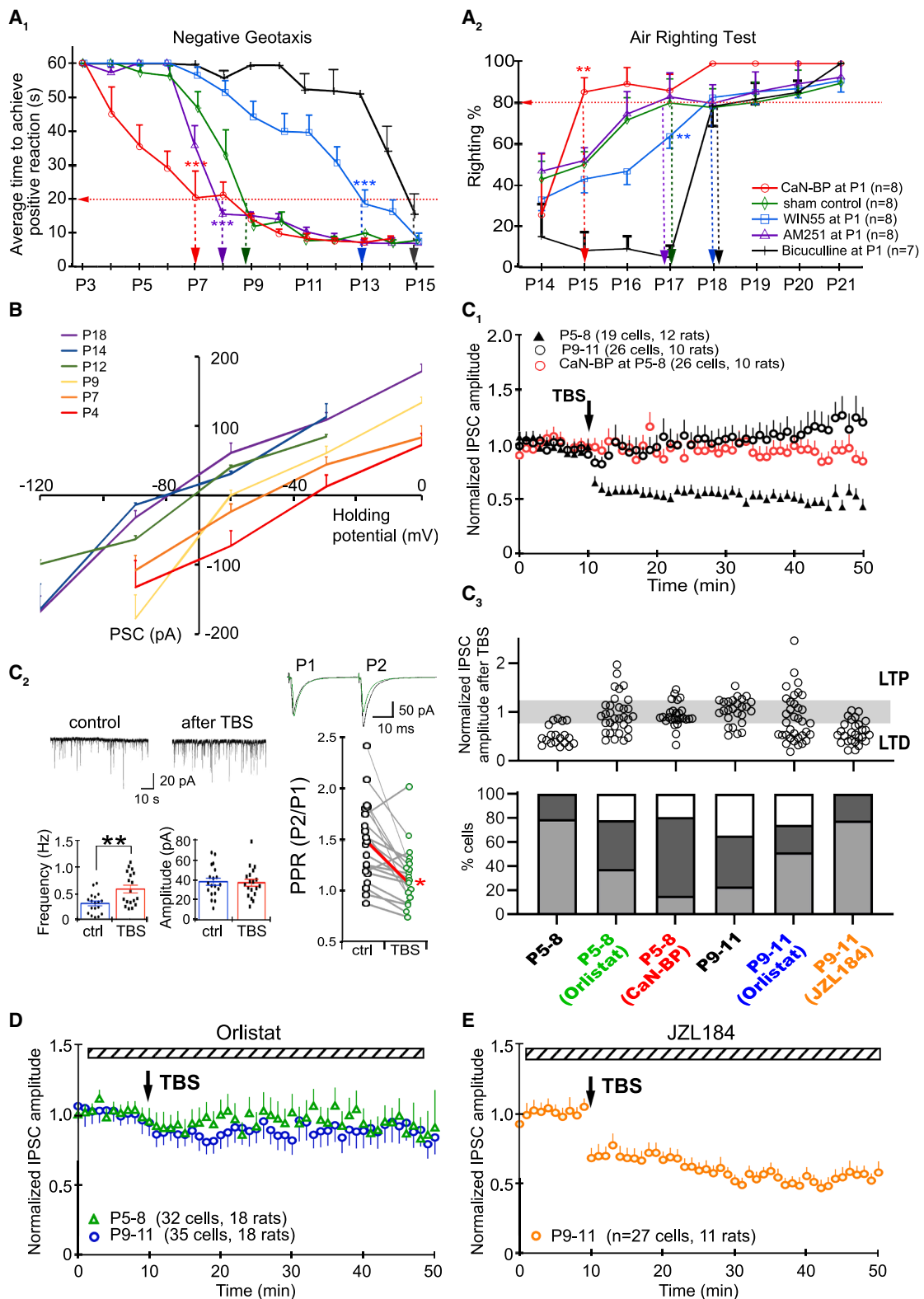
Sequential emergence of increasingly complex behavior in development involves nature-defined innate developmental programs subject to nurture resultant from experience-dependent fine-tuning of neural circuits mediated by synaptic plasticity.¹ The endocannabinoid system (eCB) plays crucial roles in modulating plastic processes that refine neural circuits based on experience.² Of particular importance is the action of the eCB system on the plasticity of gamma-aminobutyric acid (GABA)ergic transmission, which in turn sets the level of neural plasticity in neonatal brain circuits. We asked how aberrations in neonatal GABAergic transmission could lead to circuit dysfunction, manifesting as behavioral deficits in patients with perinatal overexposure to cannabinoids.³ Vestibular circuits, which undergo significant refinement in the early postnatal period,^{4–6} are most susceptible to early cannabinoid exposure.

The role of GABAergic neurons in shaping afferent input processing at second-order vestibular neurons was established by pioneering studies in the frog.^{7,8} Previously, we

showed that GABAergic transmission was required for the functional maturation of vestibular circuits,^{4,5} even with intact inputs from vestibular sensory input.⁶ In this study, we further demonstrate that type I cannabinoid receptor (CB1R) activity in the early postnatal stage sets the trajectory of synaptic plasticity at GABAergic synapses of vestibular nucleus (VN) circuits.

High synaptic plasticity in GABAergic transmission within the critical period and abrupt decrease of plasticity at the end of the critical period is a common mechanism for the fixation of synaptic characteristics in many sensory systems after a postnatal period of input-dependent refinement.^{9–11} While it is assumed that a period of heightened plasticity within the critical period allows input-guided fine-tuning of developing circuits,¹⁰ it is not known whether the temporal control of plasticity in GABAergic transmission is required for circuit maturation. In the absence of sensory input, such as during dark rearing, eCB was required for closure of the extended critical period.¹² Given omnipresent vestibular input is present in neonate^{4,13,14} and neuronal expression of CB1R since birth,¹⁵ we asked how the activity of the eCB





(legend on next page)

system early in the critical period determines the closure of the critical period.

Vestibular outputs are conveyed via distinct projection pathways segregated by function,^{13,14} with distinct output dynamics.¹⁶ This implied existence of distinct signal processing circuits within the VN. Evidence suggests that such differences in the processing of sensory inputs arise not only from differing intrinsic properties of neuronal subtypes,¹⁷ but also from differences in inhibitory inputs.⁷ On the most basic level, inhibitory synapses can be classified as inhibitory motifs when GABAergic neurons impinge on excitatory neurons, or disinhibitory motifs when both the pre- and postsynaptic neurons are inhibitory.¹⁸ By separating these two motifs during the recording of GABAergic postsynaptic currents in VGAT-Venus mice,¹⁹ we revealed type B cholecystokinin receptors (CCK_BR) and serotonin-2A receptors (5-HT₂AR) as unique physiological triggers of eCB-mediated plasticity at developing disinhibitory and inhibitory motifs, respectively.

Here, we show that early postnatal exposure to CB1R agonist delayed the maturation trajectory of GABAergic plasticity in VN circuits in rodents, with such animals suffering from long-lasting navigational deficit in adulthood. Although the role of motif-specific tuning of plasticity during the critical period remains to be elucidated, behavioral deficits resulting from overriding these triggers by the non-discriminatory stimulation of eCB receptors revealed its importance in circuit maturation. Results, therefore, highlight the importance of both temporal and motif-specific regulation of LTD_{GABA} toward the formation of functional circuits in the VN.

RESULTS

A critical period for endocannabinoid modulation of graviceptive behavior

Localized efflux of CB1R agonist WIN55 above the VN from P1 delayed the emergence of negative geotaxis to P13 (Figure 1A₁, WIN55-treated vs. sham controls, a blocking peptide against calcineurin^{20–22} (CaN-BP)- or CB1R antagonist AM251-

treated at P13: $p < 0.001$), contrasting with saline controls in which this behavior emerged by P9. The air righting reflex, which normally emerges at P17, was also delayed to P18 by such treatment (Figure 1A₂, WIN55-treated vs. all other treatments at P17: $p < 0.01$). Contrarily, exposure to AM251 from P1 advanced the emergence of negative geotaxis to P8 (Figure 1A₁, AM251-treated vs. sham controls, WIN55-, or BIC-treated at P8: $p < 0.001$). The combined treatment of WIN55 and AM251 had no significant effect on either behavioral test (Figure S2). This established that CB1R activity in the early postnatal stage bi-directionally affected the circuit maturation of the medial vestibular nucleus (MVN).

Exposure to WIN55-loaded Elvax from P12 onwards did not affect negative geotaxis (Figure S3B). This time point coincided with the switch in polarity of GABAergic transmission (E_{GABA}) in VN from depolarizing to hyperpolarizing at P12 (Figure 1B), a hallmark of the maturation of GABAergic circuits.²³ We further found that WIN55 exposure at P8, one day before the functional maturation of circuits for negative geotaxis, also caused no delay (Figure S3A). Results corroborate clinical evidence that chronic adult exposure to cannabinoids is largely inconsequential²⁴ and highlighted a critical period closing at P8 during which the CB1R directed maturation of VN circuits.

Decrease in induction efficacy of long-term depression at GABAergic synapses drives circuit maturation

Decreased synaptic plasticity of VN circuits in normal rats at P8, as reflected magnitude of long-term change in synaptic strength after TBS (Figure 1C₁), accompanied closure of the critical period for vestibular development at this stage.

Examination of individual responses revealed a significant decrease in percentage of MVN neurons displaying an LTD response after TBS, from 80% within the critical period (P5–8) to 20% after the closure of the critical period for VN circuits that support reflexive actions at P9–11 (Figure 1C₃, $p < 0.001$ vs. P5–8). The magnitude of LTD_{GABA} in cells that continued to show LTD response in P9–11 rats was also reduced compared to those in P5–8 rats ($63.46 \pm 9.03\%$, $n = 6/26$ cells, 10 rats,

Figure 1. eCB shifts the maturation program of VN circuits through tuning synaptic plasticity at GABAergic synapses

(A) The emergence of negative geotaxis (A₁) and air-righting reflex (A₂) were delayed with the pretreatment of the VN at P1 with CB1R agonist WIN55 or GABA_AR antagonist bicuculline, but advanced with CB1R antagonist AM251 or CaN-BP.

(B) Gramicidin-perforated whole-cell patch-clamp recording of GABA reversal potential. Postnatal shift of I-V curve indicated that GABAergic response of MVN neurons changed from excitatory to inhibitory between P9 and P12. Vertical axis intersects the horizontal axis at -70 mV (average resting membrane potential).

(C₁) Average response of MVN neurons to TBS in brain slices obtained from P5–8, P9–11 and P5–8 treated with CaN-BP.

(C₂) Following TBS, mPSC_{GABA} frequency was increased ($n = 19$ cells, $p < 0.001$) but amplitude was unchanged ($n = 19$ cells, $p > 0.05$) and PPR was decreased ($n = 17$ cells, $p < 0.01$), indicating presynaptic plasticity. Lines join PPR values from the same cell. Red line indicates change in mean PPR value before and after TBS. Representative tracings of paired-pulse responses before (black) and after TBS (green) are shown above.

(C₃) Top: Normalized PSC amplitudes of each recorded cell after TBS under various experimental conditions. Pale gray area denotes no change in PSC_{GABA} amplitude, the area below for LTD in PSC amplitude, and that above for LTP response. Bottom: Bar chart summarizing the percentage of MVN neurons showing LTD (light gray), LTP (white) or no change in PSC amplitude (dark gray). In P5–8 brain slices, 80% of sampled MVN neurons exhibited TBS-induced LTD_{GABA}, while the remaining 20% showed no change. LTP was not observed. With the bath addition of CaN-BP, 65% of sampled MVN neurons showed no response to TBS (red circles in C₃, $p < 0.001$ vs. untreated P5–8 cells). In P9–11 slices, the occurrence of LTD decreased to 29% while another 32% of sampled MVN neurons exhibited LTP ($p < 0.001$ vs. untreated P5–8 cells).

(D) LTD was abolished in the averaged PSC response of all recorded MVN cells in P5–8 brainstem slices after blocking lipase activity with the bath addition of Orlistat. Closer examination of the response of each cell further revealed that the proportion of LTD_{GABA}-expressing MVN neurons was significantly decreased to 38% ($p = 0.008$, vs. untreated P5–8 cells, see C₃). LTP was induced in another 22% of sampled MVN neurons.

(E) With the bath addition of JZL184 to P9–11 brainstem slices to inhibit 2-AG degradation, the percentage of MVN neurons that showed LTD_{GABA} increased to 78% ($p < 0.001$ vs. untreated P9–11 cells). Mean \pm SEM are shown. * $p < 0.05$, ** $p < 0.01$, *** $p < 0.001$. two-way ANOVA for behavioral tests in (A), pair t-test for mPSC_{GABA} recordings in (C₂), Fisher's exact test with Bonferroni's correction for multiple measurements was used to evaluate change in responses to TBS in (C₃).

$p = 0.002$) (Figure 1C₃). Addition of GABA_A receptor antagonist bicuculline to the bath after the LTD measurements confirmed that the PSCs observed were indeed mediated by GABA_A receptors (Figure S3D). These confirmed that the maturation of MVN circuits and closure of the critical period were also marked by a decrease in synaptic plasticity, as in critical periods of cortical circuits.²⁵

We then tested whether decreased LTD_{GABA} incidence could, in turn, promote the functional maturation of VN circuits. Exposure of VN neurons to CaN-BP at P1 decreased LTD_{GABA} incidence in the neonatal VN to 15% (Figure 1C, $p < 0.001$ vs. untreated). Such treatment also advanced the emergence of negative geotaxis from P9 to P7 (Figure 1A₁), and that of air righting behavior from P17 to P15 (Figure 1A₂). Contrarily, blockade of GABA_A receptors to simulate depressed GABAergic transmission resultant from sustained high LTD_{GABA} incidence, using a bicuculline-loaded Elvax slice, delayed the emergence of negative geotaxis to P15 (Figure 1A₁) and that of air righting reflex to P18 (Figure 1A₂). These results suggested that the plasticity of GABAergic transmission is causal for VN circuit maturation.

Long-term depression at GABAergic synapses in the medial vestibular nucleus during the critical period is mediated by endocannabinoid signaling

To dissect the controlling mechanism for LTD_{GABA} in the VN during the early postnatal period (P5–8), we first determined if pre- or post-synaptic mechanisms were dominant in this period. Significantly increased miniature PSC_{GABA} frequency (0.46 ± 0.03 Hz to 0.64 ± 0.04 , $n = 19$ cells, $p < 0.01$) and decreased paired pulse ratio (PPR, 1.49 ± 0.39 to 1.15 ± 0.29 , $n = 19$ cells, $p < 0.001$) after TBS (Figure 1C₂), and unchanging PSC_{GABA} amplitude (before TBS: 38.64 ± 0.82 pA, after TBS: 35.55 ± 0.91 pA, $n = 19$ cells, $p = 0.874$) pointed to the pre-synaptic regulation of GABAergic plasticity.

We therefore tested if the presynaptic CB1R receptor^{12,18,26,27} was a major regulator for synaptic plasticity in the neonatal VN. Blocking synthesis of CB1R ligand 2-arachidonoylglycerol (2-AG) with Orlistat decreased the percentage of P5–8 MVN neurons capable of expressing LTD_{GABA} from 80% (control) to 38% (Figures 1C₃ and 1D, $p = 0.008$ vs. untreated). Conversely, the inhibition of 2-AG degradation with JZL184 in P9–11 MVN neurons increased the induction efficacy of LTD_{GABA} from 29% (control) to 78% (Figures 1C₃ and 1E, $p < 0.001$ vs. untreated). It is noteworthy that JZL184 caused a decrease in membrane resistance (Figure S4). These pharmacological manipulations proved that the majority of TBS-induced LTD_{GABA} in the neonatal rat VN was elicited by activity of eCB system.

Early cannabinoid exposure prolonged high level of long-term depression induction at GABAergic synapses

If so, can CB1R activity set the developmental trajectory of decreasing LTD_{GABA} incidence? Abolishment of further LTD_{GABA} response to a second TBS by the bath addition of AM251 (Figure 2A; Figure S5) or Orlistat (Figure 2F, blue tracing) proved that the observed LTD_{GABA} was indeed mediated by CB1R. In rats pretreated with WIN55 at P1, a high incidence (79%) of eCB-mediated LTD_{GABA} (Figure 2B) was maintained to P9–11 (Figure 2E, 78%), contrasting with 23% in controls

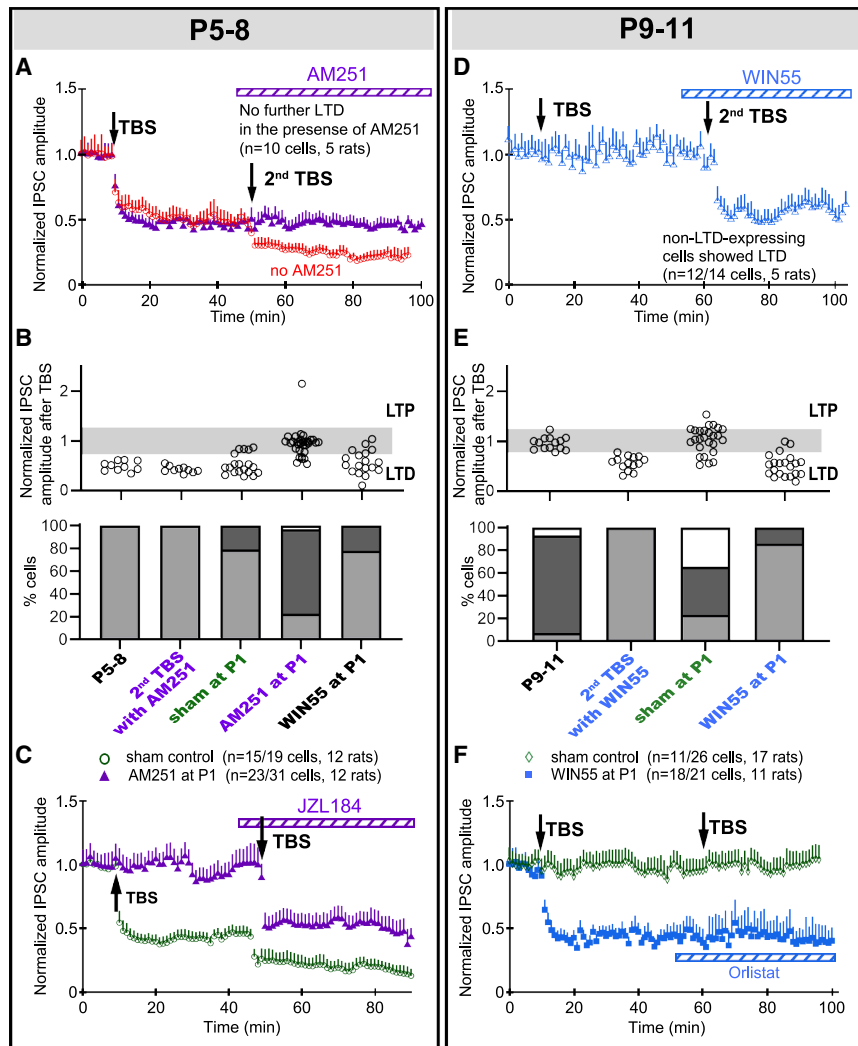
(Figure 2E, $p < 0.001$ vs. sham controls). Conversely, pre-treatment with AM251 at P1 decreased the occurrence of eCB-mediated LTD_{GABA} at P5–8 from 79% (sham) to 23% (Figure 2B, $p < 0.001$ vs. sham), indicating the premature suppression of plasticity in MVN circuits. The amplitude of LTD in cells that responded as such to TBS, however, was unchanged by pre-treatment with WIN55 at P1 ($46.84 \pm 7.83\%$, $n = 17/23$ cells, 11 rats, $p = 0.814$) or AM251 at P1 ($45.42 \pm 7.09\%$, $n = 8/41$ cells, 12 rats, $p = 0.934$) as compared to control rats.

In P9–11 rats, the lower percentage of cells showing LTD_{GABA} after TBS was not due to the developmental downregulation or inactivation of CB1R on these neurons. Using a double TBS protocol, P5–8 or P9–11 MVN neurons which did not display LTD_{GABA} after an initial TBS could be induced to display LTD_{GABA} by increasing synaptic 2-AG concentration with JZL181 (Figure 2C, purple tracing) or direct activation of CB1R with WIN55 (Figure 2D). Additionally, most recorded neurons were excitatory, and WIN55 decreased their excitability (Figure S6). This implied that the retrograde activation of CB1R by postsynaptic release of endocannabinoids was the predominant factor that governed the incidence of LTD_{GABA} in the VN.

Unique triggers for 2-arachidonoylglycerol release in medial vestibular nucleus circuits

We then tested the efficacy of other G_q-coupled receptors, such as 5-HT_{2A}R and CCK_BR,^{28,29} that were less commonly associated with 2-AG release in the forebrain.^{30,31} Bath application of 5-HT_{2A} receptor antagonist MDL11939 (Figure 3A₁) significantly decreased the probability of LTD_{GABA} incidence among P5–8 MVN neurons to 30% ($p = 0.004$), while CCK_BR antagonist CI988 (Figure 3A₂) produced a slight decrease to 50% ($p = 0.096$) (Figure 3A₄). While the same canonical PLC-, PKA-, and Ca²⁺-dependent intracellular pathways as those in forebrain neurons^{32,33} were utilized by MVN neurons to effect eCB mediated LTD_{GABA} (Figures S7A–S7C), MVN neurons utilized distinct transmembrane signaling receptors to trigger 2-AG release. In the forebrain, 2-AG release triggered by metabotropic glutamate receptor (mGluR) is well documented.^{34–36} Bath application of mGluR5 antagonist MPEP or mGluR1 antagonist LY367385 to MVN slices of P5–8 rats (Figure 3A₃), however, did not change the induction efficacy of eCB-mediated LTD_{GABA} (Figure 3A₄, MPEP, $p = 1$; LY367385, $p = 0.347$ vs. control).

Whereas in P9–11 rats, the application of 5-HT₂R agonist α -m-5-HT (Figure 3B₁) significantly increased the proportion of cells responding to TBS with LTD_{GABA} to 78% ($p < 0.001$ vs. control), while CCK (Figure 3B₂) increased the proportion to 57% ($p = 0.011$ vs. control) (summarized in Figure 3B₄). Such an increase in the proportion of cells showing LTD_{GABA} response was confirmed to be eCB-mediated by the addition of orlistat to the bath which blocked further induction of LTD_{GABA} by a second TBS in P9–11 rat VN neurons despite the presence of CCK (Figure 3B₂) or α -m-5-HT (Figure 3B₁). The apparent redundancy of 5-HT_{2A}R and CCK_BR on triggering eCB-mediated LTD_{GABA} in the MVN suggested the possibility of yet unknown mechanisms for differential control of plasticity in GABAergic transmissions. Addition of mGluR1 agonist DHPG (Figure 3B₃) also did not affect the induction of eCB-mediated LTD_{GABA} in P9–11 cells (Figure 3B₄, $p = 0.484$ vs. control). These results thus



LTD_{GABA} after the addition of Orlistat to the bath. Mean \pm SEM are shown. Fisher's exact test Bonferroni's correction for multiple measurements was used to evaluate change in responses to TBS in (B) and (E).

demonstrate that the activation of mGluR1/5 did not trigger post-synaptic release of 2-AG as a retrograde messenger necessary for the induction of eCB-mediated LTD_{GABA} in MVN, distinct from glutamate-dependent triggering eCB-mediated LTD_{GABA} in the hippocampus.³⁷

Cell-type specific control of long-term depression at GABAergic synapses by the differential triggering of endocannabinoid release

GABAergic neurons impinging upon excitatory or inhibitory neurons form inhibitory and disinhibitory motifs, respectively.¹⁸ Being the building blocks of functional circuits,¹⁸ we reasoned that the tuning of plasticity at such motifs would require distinct regulation. Use of vesicular GABA transporter (VGAT)-Venus transgenic mice¹⁹ allowed the distinction of plasticity at disinhibitory (Figure 4A₁) and inhibitory motifs (Figure 4A₂). The overall profile of TBS-induced neuronal plasticity in VGAT-Venus mice was not different from rats (P5-8 VGAT mice vs. P5-8 rat, $p =$

0.682; P9-17 VGAT-Venus mice vs. P9-11 rat, $p = 0.694$) nor from wild type mice (P5-8, $p = 0.402$; P9-17, $p = 1$).

Moreover, VGAT and non-VGAT neurons had similar incidence of LTD_{GABA} (P5-8, $p = 0.538$; P9-17, $p = 0.873$, Figures 4A_{1,2}, and 4G_{1,2}), which were reduced with age (VGAT neurons, $p < 0.001$; non-VGAT neurons $p = 0.033$). The amplitude of LTD_{GABA} after TBS was also similar between VGAT-Venus and rats (P5-8, $p = 0.779$; P9-17, $p = 0.580$). Addition of Orlistat could abolish further induction of LTD_{GABA} in both VGAT (Figure 4C₁) and non-VGAT cells (Figure 4C₂) in P5-8 MVN VGAT-mice. These confirm the validity of VGAT-Venus mice as a model for studying LTD_{GABA} in the MVN during early postnatal development.

We revealed the differential modulation of LTD_{GABA} incidence at VGAT versus non-VGAT neurons by the bath addition of 5-HT_{2A}R or CCK_BR agonists/antagonists. In P5-8 MVN slices, the bath addition of 5-HT_{2A}R antagonist MDL11939 did not change the induction efficacy of LTD_{GABA} in VGAT neurons compared to untreated controls (Figures 4D₁ and 4F₁, $p = 0.560$), but such

Figure 2. eCB system governs the induction efficacy of LTD_{GABA} and sets the developmental trajectory of LTD_{GABA} in developing VN neurons

(A) In P5-8 brain slices, MVN neurons that responded to an initial TBS with LTD_{GABA} could no longer respond to a second TBS with further LTD_{GABA} after the bath addition of AM251 (purple triangles). In a parallel preparation of P5-8 slices (red circles), a second TBS could induce further LTD_{GABA} in LTD_{GABA}-expressing MVN neurons.

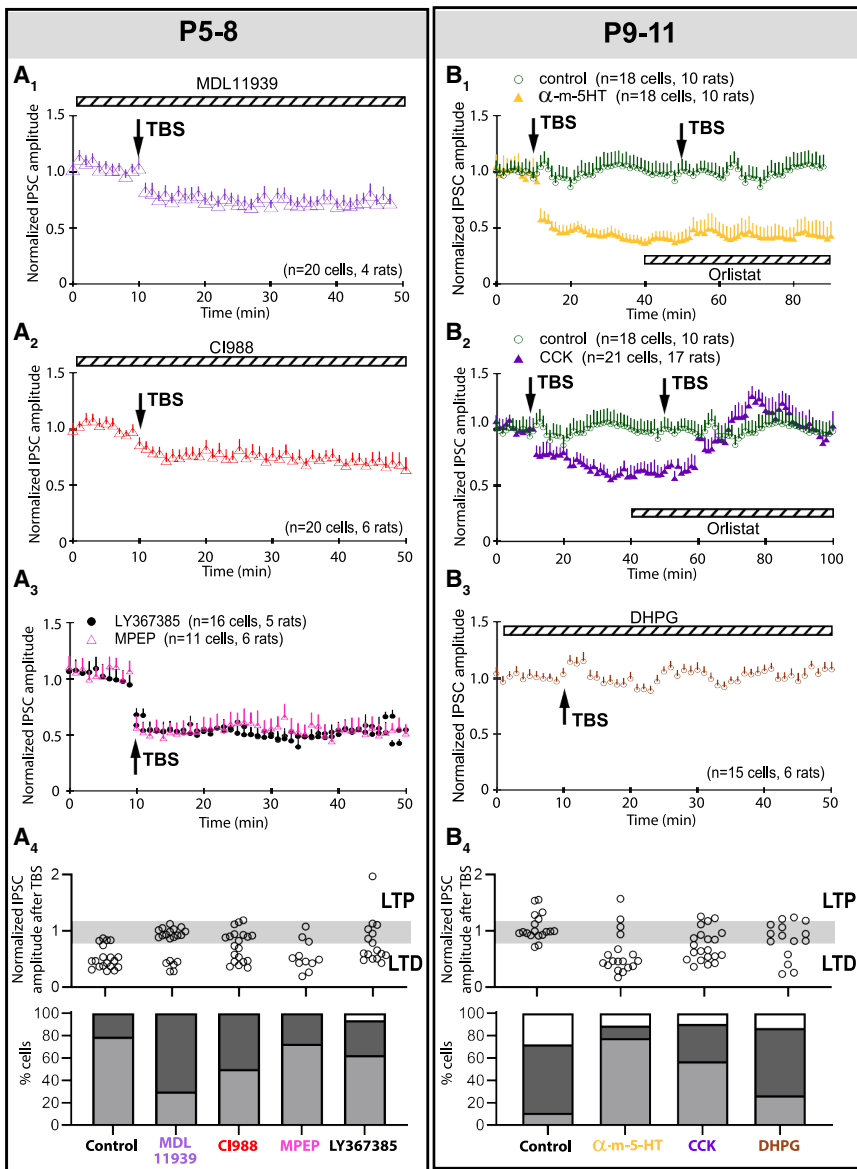
(B) Bar charts summarizing the individual PSC_{GABA} (top) and the percentages (bottom) of P5-8 MVN neurons to TBS after sham or P1 a.m.251 application, as well as the percentage of cells showing each type of response, viz. LTD (light gray), LTP (white) or no change in PSC amplitude (dark gray).

(C) In P5-8 rats pre-treated with AM251 at P1, 74% of sampled MVN neurons in brain slices did not exhibit LTD_{GABA} following an initial TBS (purple triangles), contrasting sham control rats in which 79% of sampled neurons showed LTD_{GABA} (green circles, $p < 0.001$). With the bath addition of JZL184, a second TBS could induce LTD_{GABA} in 80% of sampled MVN neurons that were non-LTD_{GABA}-expressing with the first TBS (purple triangles).

(D) In P9-11 slices, all sampled MVN neurons that did not respond to an initial TBS could then be induced to express LTD_{GABA} with a second TBS after the bath addition of WIN55.

(E) Bar charts summarizing the individual PSC_{GABA} (top) and the percentages (bottom) of P9-11 MVN neurons to TBS after sham or P1 WIN55.

(F) In P9-11 rats pre-treated with WIN55 (blue squares) at P1, 86% of sampled MVN neurons in brain slices exhibited LTD_{GABA} after the first TBS, contrasting sham control rats in which only 23% of sampled MVN neurons showed LTD_{GABA} ($p < 0.001$). These LTD_{GABA}-expressing cells could not respond to a second TBS with further



TBS. Mean \pm SEM are shown. Fisher's exact test with Bonferroni's correction for multiple measurements was used to evaluate change in responses to TBS in (A₄) and (B₄).

treatment reduced LTD_{GABA} incidence to 17% in non-VGAT neurons (Figure 4D₂, $p = 0.008$). While the effect of CI988 was not significant in random patch-clamp recordings of MVN neurons (cf. Figure 4A₂), cell type-specific recording in P5-8 VGAT-Venus mice revealed that CCK_BR antagonist CI988 significantly decreased the probability of LTD_{GABA} induction from 94% to 50% in VGAT neurons (Figures 4E₁ and 4G₁, $p = 0.009$), but not in non-VGAT neurons (Figures 4E₂ and 4G₁, $p = 0.294$). Additionally, the combined bath application of MDL11939 and CI988 did not suppress LTD_{GABA} induction more effectively than either antagonist alone (Figure S8).

Distinct triggering of eCB-mediated plasticity at inhibitory and disinhibitory motifs persisted after closure of the critical

Figure 3. eCB release is triggered by 5-HT and CCK receptors but not metabotropic glutamate receptors in developing VN neurons

(A₁) With the bath addition of MDL11939 (a 5-HT receptor antagonist) to P5-8 brain slices, the percentage of P5-8 MVN neurons showing LTD_{GABA} decreased to 30% (green triangles, $p = 0.003$), contrasting 79% in controls.

(A₂) With the bath addition of CI988 (a CCKBR antagonist) the percentage of P5-8 MVN neurons showing LTD_{GABA} decrease slightly to 50% (CI988, blue triangles), but was not statistically significant ($p = 0.096$).

(A₃) With the bath addition of LY367385 (a mGluR1 receptor antagonist, black circles) or MPEP (a mGluR5 antagonist, pink triangles), the percentage of P5-8 MVN neurons showing LTD_{GABA} was similar to the control (LY367385: 73%, $p = 1$; MPEP: 62%, $p = 0.347$).

(A₄) Bar charts summarizing the individual PSC_{GABA} (top) and the percentages (bottom) of P5-8 MVN neurons showing each type of response (LTD, light gray; LTP, white; no change, dark gray) in each treatment group after TBS.

(B₁) In P9-11 brain slices, no LTD or LTP was observed in the averaged response of recorded MVN cells (green circles). This was in agreement with the majority (61%) of cells showing no change after TBS (see B₄). With the bath addition of α-m-5-HT (a 5-HT receptor agonist), the percentage of MVN neurons showing LTD_{GABA} after an initial TBS increased to 78% (yellow triangles, $p < 0.001$). These LTD_{GABA}-expressing cells could not respond to a second TBS with further LTD_{GABA} with the addition of Orlistat to the bath.

(B₂) With the bath addition of CCK (a CCKBR agonist), 57% of the P9-11 MVN neurons showed LTD_{GABA} (purple triangles, $p = 0.011$), contrasting control rats in which only 11% of sampled MVN neurons showed LTD_{GABA}.

(B₃) With the bath addition of DHPG (a mGluR1 agonist), the percentage of MVN neurons showing LTD_{GABA} after TBS did not change significantly (27%, blue circles, $p = 0.484$).

(B₄) Bar charts summarizing the individual PSC_{GABA} (top) and the percentages (bottom) of P9-11 MVN neurons in each treatment group after

period. In P9-17 MVN, 5-HT remained as a trigger for LTD_{GABA} in non-VGAT neurons. Increasing the proportion of LTD_{GABA} responses from 20% to 87% ($p = 0.001$, Figure 4F₂) but not in VGAT neurons (from 20% to 19%, $p = 0.227$, Figure 4F₂). On the other hand, the bath addition of CCK continued to increase the proportion of cells responding to TBS with LTD_{GABA} in VGAT neurons (from 31% to 73%, $p = 0.004$, Figures 4F₁ and 4G₂) but not non-VGAT neurons (from 20% to 31%, $p = 0.857$, Figures 4F₂ and 4G₂). In all, results revealed that the triggering of LTD_{GABA} in non-VGAT neurons was 5-HT_{2A}R-dependent while that in VGAT neurons was CCK_BR-dependent (Figure 4H), and this phenomenon is calcium-independent (Figure S9).

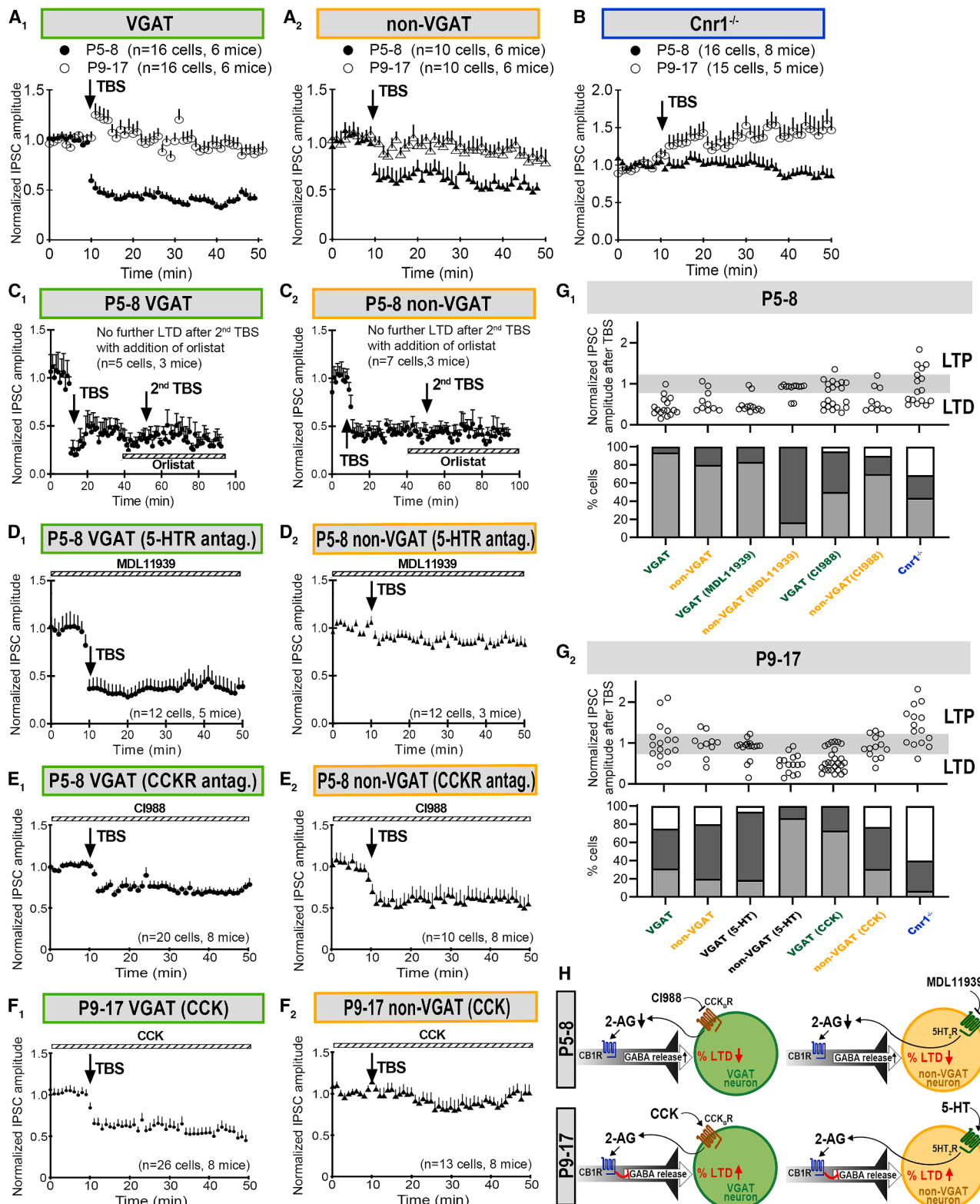


Figure 4. Distinct triggers for eCB-mediated LTD_{GABA} at inhibitory and excitatory neurons in VN

(A) In P5-8 VGAT mice (filled circles), the majority of sampled VGAT (A₁, 40%) and non-VGAT neurons (A₂, 80%) in the MVN showed LTD_{GABA} after TBS. While at P9-17 (open circles), the majority of neurons showing no change in response amplitude after TBS (A₂).

(legend continued on next page)

Long-term plasticity in cannabinoid receptor 1 knock-out mice

The role of eCB system on GABAergic synaptic transmission and plasticity was further confirmed using CB1R knock-out ($\text{Cnr1}^{-/-}$) mice. The amplitude of miniature $\text{IPSC}_{\text{GABA}}$ was similar between control and knockout mice both at P5–8 (Figure 5A_{1,2}, $p = 0.14$) and P9–17 (Figure 5B_{1,2}, $p = 0.83$). Decay time of $\text{mPSC}_{\text{GABA}}$ was shorter in P5–8 $\text{Cnr1}^{-/-}$ mice compared to controls (Figure 5A₂, $p = 0.037$). The frequency of $\text{mPSC}_{\text{GABA}}$ in $\text{Cnr1}^{-/-}$ mice was significantly lower than age-matched controls (Figures 5A₂ and 5B₂, P5–8: $p = 0.014$, P9–17: $p = 0.04$) with longer inter-event interval (Figures 5A₁ and 5B₁, $p = 0.03$) throughout the period investigated (P5–17). This decreased probability of GABA release suggested less depression of GABAergic transmission in $\text{Cnr1}^{-/-}$ mice. Moreover, significantly increased PPR in $\text{Cnr1}^{-/-}$ mice throughout this period compared to controls (Figures 5A₂ and 5B₂, P5–8: $p < 0.0001$, P9–17: $p < 0.0001$) supported the notion of a presynaptic site of action for CB1R.

Whole-cell patch-clamp recording from MVN neurons in $\text{Cnr1}^{-/-}$ mice further confirmed the role of CB1R on LTD_{GABA} induction. Incidence of LTD_{GABA} was significantly lower in P5–8 $\text{Cnr1}^{-/-}$ mice (44% in $\text{Cnr1}^{-/-}$, Figure 4G₁) compared to VGAT-Venus mice (88%, $p = 0.001$). After the maturation of VN circuits at P9–17, incidence of LTD_{GABA} was no longer different between $\text{Cnr1}^{-/-}$ (7%, Figure 4F₂) and VGAT-Venus mice (27%, $p = 0.07$) mice after the maturation of VN circuits. These results highlight the importance of CB1R in controlling LTD_{GABA} response among developing VN circuits.

Long-lasting effects of neonatal perturbation of type I cannabinoid receptor in the vestibular nucleus on the maturation of spatial navigation

Direct dosing of CB1R agonist and antagonist bypassed motif-specific regulatory mechanisms for 2-AG release, with corresponding alteration to the duration of the neonatal period of high induction efficacy of LTD_{GABA} , and were accompanied by shifts in the maturation of MVN circuits for reflexes. Given that VN outputs also inform spatial cognition, we reasoned that the perturbed maturation of MVN circuits further impacts multimodal functions such as spatial cognition.¹⁴ The dead reckoning test was used to assess the spatial cognition of adult rats³⁸

(Figure S10). In the dark probe test, where visual signals are absent, vestibular signals become the dominant sensory input for navigational behavior.³⁸ Sham control rats acquired the task significantly faster than adult rats pretreated with WIN55 at P1 (Figure 6E, $p < 0.01$). Analysis of the pattern of homeward paths of all WIN55-pretreated rats (Figure 6A, third column from the left), revealed deficits in homeward navigation (i.e., increase in heading angle, time spent in the food quadrant, and error in locating the homebase) in the dark ($p < 0.01$ for all parameters). Normal performance of these rats in the light probe test supported a vestibular origin for the deficit (Figures 6B–6D). Early suppression of LTD_{GABA} induction efficacy with CaN-BP (Figure 1C) or AM251 pretreatment at P1 (Figure 2B) did not cause navigational impairment in either the light or dark probe test (Figures 6A–6D). However, when spatial memory played a more significant role, such as when presented with conflicting visual and vestibular cues in the new location test, both WIN55- and AM251-pretreated rats had difficulty finding their way back to the new home (Figures 6A–6D).

Absence of navigational deficits both in the light and dark probe tests despite perturbation with WIN55 or AM251 at P8 or P12 implied the normal operation of adult circuits for processing visual and vestibular inputs (Figures S11 and S12). This demonstrated that the critical period for vestibular-dependent navigation was also closed by P8.

DISCUSSION

Retardation of neurodevelopment by early exposure to cannabinoids has been documented³ but the mechanism of this has remained unclear. By following the maturation of the vestibular system in the early postnatal stage, this study provides evidence that control of LTD_{GABA} by CB1R is crucial not only for the timely maturation of local reflexive circuits in the MVN but also permanent establishment of vestibular-dependent higher functions such as navigation. We revealed specific triggers for LTD_{GABA} at inhibitory and disinhibitory motifs within the MVN. Bypassing these triggers with the non-discriminatory activation of presynaptic CB1R in the early postnatal period sustained high occurrence of plasticity in GABAergic transmission beyond the normal duration of the critical period. This led to delayed postnatal

(B) $\text{Cnr1}^{-/-}$ mice had higher percentage of LTP-expressing MVN neurons at both P5–8 (filled triangles, $p = 0.001$), but the difference was no longer significant at P9–17 (open circles, $p = 0.067$) compared with VGAT-Venus mice.

(C) In P5–8 mice, LTD_{GABA} -expressing neurons in both VGAT (C₁) and non-VGAT (C₂) populations could not be induced to express LTD_{GABA} with a second TBS after the bath addition of Orlipstat.

(D) Bath addition of MDL11939 (a 5HT_{2A}R antagonist) to P5–8 brain slices did not affect LTD_{GABA} in VGAT neurons in the MVN ($p = 0.560$) (D₁). However, the percentage of LTD-expressing non-VGAT cells was significantly decreased to 17% ($p = 0.008$) after the bath addition of MDL11939 (D₂).

(E₁) With the bath addition of Cl988 (a CCK_BR antagonist) to P5–8 slices, the percentage of LTD_{GABA} -expressing VGAT neurons in the MVN decreased to 50% ($p = 0.009$ vs. P5–8 control).

(E₂) Such treatment did not significantly reduce the percentage of LTD_{GABA} -expressing non-VGAT neurons in the MVN (70%, $p = 0.293$).

(F₁) With the bath addition of CCK to P9–17 slices, the percentage of LTD_{GABA} -expressing VGAT neurons in the MVN was increased to 73% ($p = 0.004$ vs. P9–17 control).

(F₂) On the other hand, the percentage of non-VGAT neurons responding to TBS with LTD_{GABA} remained similar to controls at 31% ($p = 0.857$).

(G_{1,2}) Bar charts summarizing PSC_{GABA} amplitudes of each recorded cell and percentages of MVN neurons showing the response described above for P5–8 (F₁) and P9–17 (F₂) VGAT-Venus and $\text{Cnr1}^{-/-}$ mice.

(H) Schematic diagram showing differential control of eCB-mediated LTD_{GABA} by CCK_BR and 5HT_{2A}R at VGAT and non-VGAT neurons in the P5–8 and P9–17 MVN. Mean \pm SEM are shown. Fischer's exact test with Bonferroni's correction for multiple measurements was used to compare response profiles to TBS between various treatment groups.

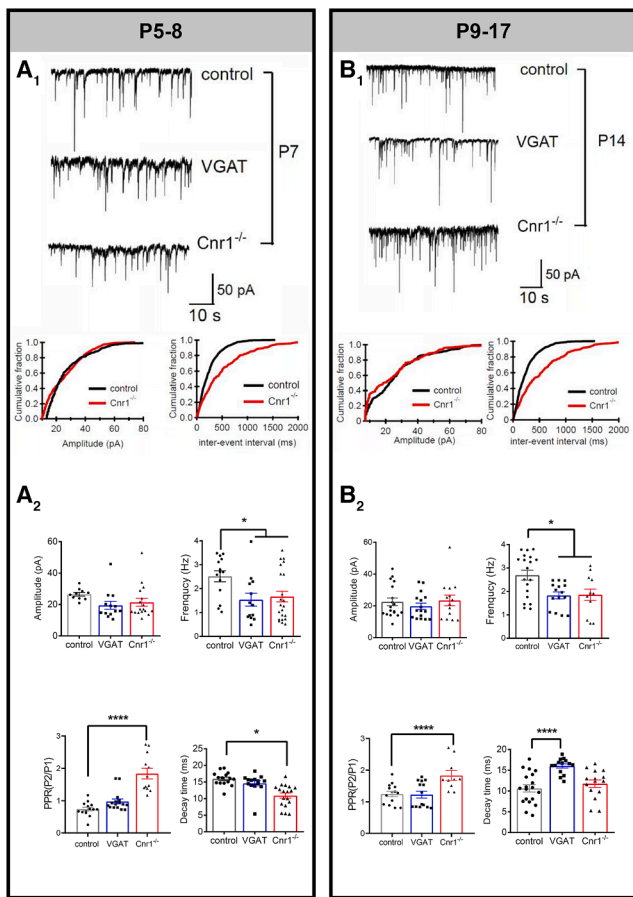


Figure 5. Use of $Cnr1^{-/-}$ to show that GABA release from VN neurons is limited by CB1R. mPSC_{GABA} of MVN cells from control, VGAT and $Cnr1^{-/-}$ transgenic mice of two age groups, viz. P5-18 and P9-17

(A₁ and B₁) *Upper panels*: Representative tracings of mPSC_{GABA} from P7 (A₁) and P14 (B₁) neurons voltage clamped at -70 mV. *Lower panels*: Cumulative distribution of amplitude and inter-event interval of mPSC_{GABA} from control (black line) and $Cnr1^{-/-}$ mice (red line).

(A₂ and B₂) The mPSC_{GABA} amplitude of MVN neurons was similar between all groups at both ages, but the mPSC_{GABA} frequency and PPR of MVN neurons was significantly increased in $Cnr1^{-/-}$. This suggested a presynaptic site of action for $Cnr1^{-/-}$. Decay time of mPSC_{GABA} was significantly shorter in $Cnr1^{-/-}$ mice of the P5-8 group but was not different at P9-17 group. Mean \pm SEM are shown. $*p < 0.05$, $***p < 0.0001$. K-S test to compare cumulative distributions in (A₁) and (B₁), two-way ANOVA for comparison of mPSC_{GABA} properties in (A₂) and (B₂).

emergence of vestibular-dependent reflexes and deficits in adult spatial cognitive performance. Taken together, the results provide a mechanistic link between early cannabinoid exposure and neurodevelopmental deficits.

Bidirectional impact of neonatal endocannabinoid system activity on maturation profile of graviceptive reflexes

GABAergic neurons play a key role in the processing of afferent inputs in VN circuits.⁵⁻⁸ While temporal control of key electrophysiological events, such as excitatory-inhibitory switch of

GABAergic transmission in the forebrain³⁹ are known to affect maturation, the contribution of temporal control of the plasticity in GABAergic transmission remains unclear. We show that long-term plasticity in GABAergic transmission within the MVN circuits is attenuated by the end of the critical period at P8, similar to other sensory systems.^{11,40,41} This, in theory, allows higher levels of depolarizing GABAergic transmission to provide the excitatory drive for the consolidation of neuronal circuits,^{23,42,43} as well as prevent further activity-dependent pruning of synapses.

CB1R activity is known to be subject to homeostatic regulation, including decreased receptor expression⁴⁴ and phosphorylation of the cytoplasmic tail of the receptor upon repeated dosing of WIN55 over a few days.^{45,46} However, such desensitization is dependent on both age and brain location, with cerebellar neurons of adolescent rats showing non-significant levels of desensitization after prolonged cannabinoid dosing.⁴⁷ While desensitization was not investigated in this study, the desensitization of CB1R in MVN after WIN55 dosing, if present, would further highlight the sensitivity of early postnatal M VN circuit to transient perturbations in CB1R activity.

In addition, we have observed that P9-17 $Cnr1^{-/-}$ mice expressed LTP in MVN neurons (Figure 4B; Figure S13). This suggests that normal CB1R activity is critical for the timely regulation of LTD_{GABA} and, by extension, for the proper development of vestibular circuits. Furthermore, the absence of CB1R disrupts the balance between LTP and LTD, which normally helps to refine synaptic connections during development.¹ LTP in these mice might result from an unregulated, excessive excitatory drive or from compensatory mechanisms due to the loss of CB1R-mediated inhibition. This unregulated plasticity could disrupt normal circuit development, potentially mirroring or exaggerating the effects seen with early cannabinoid exposure.

Interestingly, decay time of mPSC_{GABA} was shorter in P5-8 $Cnr1^{-/-}$ mice compared to controls (Figure 5A). Presynaptic CB1 receptors influence postsynaptic response as evidence show that endocannabinoids selectively inhibit a subclass of synapses distinguished by their fast kinetics and large unitary conductance.⁴⁸ $Cnr1^{-/-}$ mice which lack CB1 receptors might lead to compensatory changes in the expression or subtype composition of GABA receptors. There might be an increase in the expression of GABA_A receptor subtypes that have faster desensitization kinetics, which could contribute to the shorter decay time.

5-HT_{2A}R and CCK_BR are involved in the retrograde regulation of long-term depression induction in vestibular nucleus

Having established a role for eCB in modulating the development of early postnatal MVN, we further asked how eCB release itself is regulated to suit circuit-specific needs. MVN neurons utilize 5-HT_{2A} and CCK_B receptors to trigger activity-dependent release of 2-AG instead of the more common mGluR. These dual triggers allowed LTD_{GABA} at disinhibitory motifs to be modulated specifically by CCK_BR, whereas that at inhibitory motifs by 5-HT_{2A}R. Thus far, inhibitory dynamics have only been described for second order VN neurons in the mature animal,^{7,8,49} with little known about the function and maturation processes of

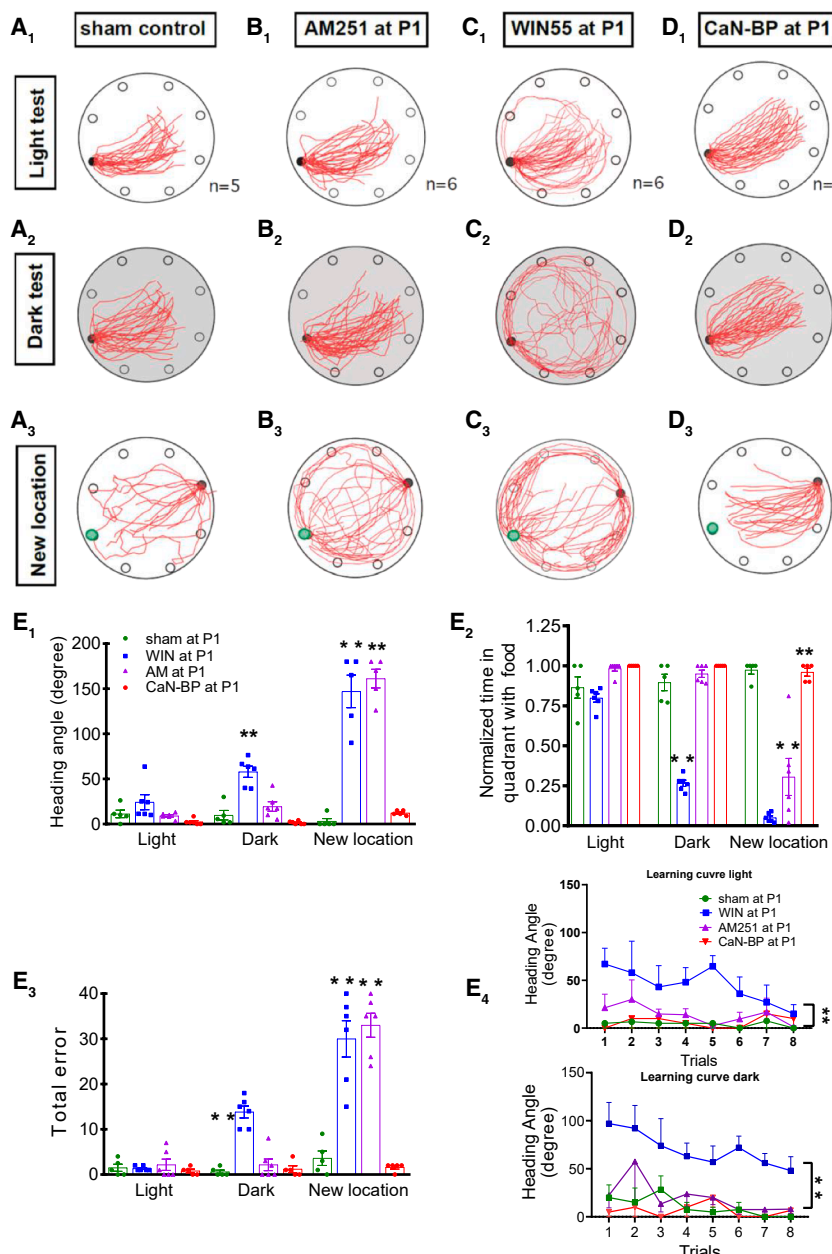


Figure 6. Perturbation of eCB signaling in the neonatal VN leads to long-lasting deficits in vestibular-dependent navigation

(A) Excursion paths of adult rats pretreated at P1 with sham implantation, AM251, WIN55, or CaN-BP in the light, dark and new location test for spatial reckoning. Red lines represent the trajectories of homeward paths (light/dark test: 8 trails/rat are superimposed; new location: 4 trials/rat are superimposed). Filled black circle on the edge of each round table surface represents the location of the home base; green circles in bottom panels represent the location of the old home base. Histograms showing the average heading angle (B), time spent in the quadrant containing food (C), errors made in locating the homebase (D), and training time required for rats pretreated with AM251 ($n = 6$ rats), WIN55 ($n = 6$ rats), CaN-BP ($n = 5$ rats), or sham operated ($n = 5$ rats) at P1 or P12 (E). Means \pm SEM are shown. * $p < 0.05$, ** $p < 0.01$, two-way ANOVA for comparison of behavioral test performance in (B–E).

development of the vestibular circuits and proper sensory processing. With early cannabinoid exposure, this coordination is disrupted. The failure to synchronize CCK and 5-HT activity properly results in improper circuit formation and associated behavioral deficits.

Effects of neonatal exposure to AM251 and WIN55 on spatial navigation

The vestibular nucleus, a key part of this system, integrates signals from the inner ear and sends them to various brain regions to help controlling reflexes and movements.⁵⁴ Neurons in the VN involves processes LTD at synapses, which helps fine-tune the responses of vestibular circuits.⁵⁵ As revealed in our findings, early eCBs exposure disrupts this plasticity, leading to the impaired development of navigation, which may manifest as problems with coordination and movement

disinhibitory motifs within the VN. Due to non-specific depolarization resultant from bipolar electrode stimulus and the placement of electrodes at the medial margin of the MVN,^{50,51} GABA-on-GABA inputs to the VN such as those from commissural inhibition,⁴⁹ ipsilateral GABAergic neurons outside the VN similar to those for glycinergic inputs,⁵² or local VN interneurons could not be differentiated. Nonetheless, results revealed a layer of complexity for plasticity in the processing of vestibular information beyond previously reported synaptic plasticity in excitatory inputs to GABAergic versus non-GABAergic VN neurons.⁵³

In a normal developing system, CCK and 5-HT work in a coordinated manner to regulate LTD_{GABA} at inhibitory and excitatory synapses, respectively. This coordination ensures a balanced

in adulthood. Vestibular cues form the basis for the relevant integration of visual information into higher circuits that guide spatial navigation.^{56–58}

While behavior-dependent recruitment of distinct subpopulations of MVN neurons to various vestibulo-thalamocortical pathways, and more importantly molecular or electrophysiological evidence for distinct critical periods in such subpopulations, remains to be provided. Our observations provided behavioral evidence supporting a later closure date in critical periods of VN neurons that support higher centers involved in more complex multi-modal tasks compared to those supporting reflexive actions. Given real world tasks are more complex than standardized behavioral tests, the sensitivity period toward cannabinoid

exposure might extend even longer into the juvenile stage in humans.

Taken together, we show that neonatal exposure to cannabinoid agonists impacted sensorimotor function in rodents, particularly causing spatial cognitive deficits that persisted into adulthood. Our work unveils specific molecular and cellular mechanisms for the eCB-mediated regulation of the induction efficacy of LTD_{GABA}, necessary for the choreographed entrainment of developing MVN circuits. The existence of motif-specific triggers for eCB-mediated plasticity opens avenues toward understanding how eCB modulates network dynamics and behavioral learning. These regulatory mechanisms of plasticity hold the keys to potential therapies that target dysregulated plasticity commonly found in neuropsychiatric disorders.

Limitations of the study

The origin of GABA-on-GABA inhibitory inputs was not revealed under the current stimulation paradigm. Nonetheless, results revealed a layer of complexity for plasticity in the processing of vestibular information beyond previously reported synaptic plasticity in excitatory inputs to GABAergic versus non-GABAergic VN neurons.

Behavior-dependent recruitment of distinct subpopulations of MVN neurons to various vestibulo-thalamocortical pathways remains unclear. More importantly, molecular or electrophysiological evidence for distinct critical periods in such subpopulations awaits further investigation. Our observations provided behavioral evidence that VN neurons that support higher centers involved in complex multi-modal tasks have a later closure date in critical periods as compared to those supporting reflexive actions. Given that real world tasks are more complex than standardized behavioral tests, we expect the sensitivity period to exogenous cannabinoid exposure to extend into the juvenile stage in humans.

RESOURCE AVAILABILITY

Lead contact

Further information and requests for resources should be directed to and will be fulfilled by the lead contact, Ying-Shing Chan (yschan@hku.hk).

Materials availability

This study did not generate new materials.

Data and code availability

- Raw data may be obtained from the corresponding author upon reasonable request.
- No code was generated from this work.
- All reagents, chemicals, and behavioral apparatus were either obtained commercially or could be assembled according to the methods using freely available materials.

ACKNOWLEDGMENTS

We thank Professor Yuchio Yanagawa for VGAT-Venus mice; Simon S.M. Chan for constructing the setups for negative geotaxis, air righting reflex, dead reckoning test, and *in vitro* electrophysiological recording; Alice Y.Y. Lui, Tony Xiaotong Liang and Florence Yu Sum Keung for assistance in the preparation of Elvax and behavioral tests; Kimmy F.L. Tsang for assistance with histology and radioisotope work. This work was funded by Beijing Natural Science Foundation (Grant No. Z200024, Z240011 and L222097 to W.S.),

Beijing Hospital Authority Clinical Medicine Development Special Fund (ZLRK202333 to W.S.), Hong Kong Research Grants Council (GRF 761812 to D.K.Y.S. and Y.S.C.), HMRF Grant (06172866 to K.L.K.W. and Y.S.C.), State Key Laboratory of Brain and Cognitive Sciences, HKU, and the Chi Lin Kok Ng BHL Foundation.

AUTHOR CONTRIBUTIONS

W.S., K.L.K.W., C.W.M., D.K.Y.S., and Y.S.C. designed the study. W.S., M.Y., F.P.B., and H.J.H. performed electrophysiological recordings. W.S., K.L.K.W., O.W.H.C., H.J.H., K.P.N., U.T.F.L., and K.W.T. performed behavioral experiments. W.S. and O.W.H.C. conducted immunohistological experiments. K.L.K.W., C.W.M., O.W.H.C., K.W.T., and Y.S.C. designed, made, and implanted the Elvax slices. W.S., M.Y., F.P.B., and Y.S.C. analyzed the electrophysiological data. W.S., K.L.K.W., C.W.M., D.K.Y.S., and Y.S.C. analyzed the behavioral data. W.S. wrote the first draft of the article. K.L.K.W., D.K.Y.S., and Y.S.C. wrote and edited the article. D.K.Y.S., and Y.S.C. conceptualized and supervised the study. W.S., K.L.K.W., D.K.Y.S., and Y.S.C. were responsible for securing funding for this study.

DECLARATION OF INTERESTS

The authors declare that they have no competing interests.

STAR METHODS

Detailed methods are provided in the online version of this paper and include the following:

- KEY RESOURCES TABLE
- EXPERIMENTAL MODEL AND STUDY PARTICIPANT DETAILS
 - Animals
- METHOD DETAILS
 - Surgery implantation of Elvax slice
 - Dead reckoning behavioral test
 - Patch clamp recording
- QUANTIFICATION AND STATISTICAL ANALYSIS

SUPPLEMENTAL INFORMATION

Supplemental information can be found online at <https://doi.org/10.1016/j.isci.2025.112566>.

Received: March 12, 2024

Revised: February 10, 2025

Accepted: April 28, 2025

Published: April 30, 2025

REFERENCES

1. Belsky, J., and Pluess, M. (2009). The nature (and nurture?) of plasticity in early human development. *Perspect. Psychol. Sci.* 4, 345–351. <https://doi.org/10.1111/j.1745-6924.2009.01136.x>.
2. Chevaleyre, V., and Castillo, P.E. (2003). Heterosynaptic LTD of hippocampal GABAergic synapses: a novel role of endocannabinoids in regulating excitability. *Neuron* 38, 461–472. [https://doi.org/10.1016/s0896-6273\(03\)00235-6](https://doi.org/10.1016/s0896-6273(03)00235-6).
3. Hurd, Y.L., Manzoni, O.J., Pletnikov, M.V., Lee, F.S., Bhattacharyya, S., and Melis, M. (2019). Cannabis and the developing brain: Insights into its long-lasting effects. *J. Neurosci.* 39, 8250–8258. <https://doi.org/10.1523/JNEUROSCI.1165-19.2019>.
4. Lai, S. K., Lai, S.-K., Wu, K.L.K., Ma, C.-W., Ng, K.-P., Hu, X.-Q., Tam, K.-W., Yung, W.-H., Wang, Y.T., Wong, T.P., Shum, D.K.-Y., et al. (2023). Timely insertion of AMPA receptors in developing vestibular circuits is required for manifestation of righting reflexes and effective navigation.

Prog. Neurobiol. 221, 102402. <https://doi.org/10.1016/j.pneurobio.2023.102402>.

5. Jiang, Q., Wu, K.L.-K., Hu, X.-Q., Cheung, M.-H., Chen, W., Ma, C.-W., Shum, D.K.-Y., and Chan, Y.S. (2024). Neonatal GABAergic transmission primes vestibular gating of output for adult spatial navigation. *Cell Mol. Life Sci.* 81, 147. <https://doi.org/10.1007/s00018-024-05170-x>.
6. Ma, C.W., Kwan, P.Y., Wu, K.L.K., Shum, D.K.Y., and Chan, Y.S. (2019). Regulatory roles of perineuronal nets and semaphorin 3A in the postnatal maturation of the central vestibular circuitry for graviceptive reflex. *Brain Struct. Funct.* 224, 613–626. <https://doi.org/10.1007/s00429-018-1795-x>.
7. Pfanzelt, S., Rössert, C., Rohrger, M., Glasauer, S., Moore, L.E., and Straka, H. (2008). Differential dynamic processing of afferent signals in frog tonic and phasic second-order vestibular neurons. *J. Neurosci.* 28, 10349–10362. <https://doi.org/10.1523/JNEUROSCI.3368-08.2008>.
8. Biedendorf, S., Malinvaud, D., Reichenberger, I., Pfanzelt, S., and Straka, H. (2008). Differential inhibitory control of semicircular canal nerve afferent-evoked inputs in second-order vestibular neurons by glycinergic and GABAergic circuits. *J. Neurophysiol.* 99, 1758–1769. <https://doi.org/10.1152/jn.01207.2007>.
9. Reh, R.K., Dias, B.G., Nelson, C.A., 3rd, Kaufer, D., Werker, J.F., Kolb, B., Levine, J.D., and Hensch, T.K. (2020). Critical period regulation across multiple timescales. *Proc. Natl. Acad. Sci. USA* 117, 23242–23251. <https://doi.org/10.1073/pnas.1820836117>.
10. Hensch, T.K. (2004). Critical period regulation. *Annu. Rev. Neurosci.* 27, 549–579. <https://doi.org/10.1146/annurev.neuro.27.070203.144327>.
11. Takeyan, A.E., and Hensch, T.K. (2013). Balancing plasticity/stability across brain development. *Prog. Brain Res.* 207, 3–34. <https://doi.org/10.1016/B978-0-444-63327-9.00001-1>.
12. Jiang, B., Huang, S., de Pasquale, R., Millman, D., Song, L., Lee, H.K., Tsumoto, T., and Kirkwood, A. (2010). The maturation of GABAergic transmission in visual cortex requires endocannabinoid-mediated LTD of inhibitory inputs during a critical period. *Neuron* 66, 248–259. <https://doi.org/10.1016/j.neuron.2010.03.021>.
13. Basaldella, E., Takeoka, A., Sigris, M., and Arber, S. (2015). Multisensory Signaling Shapes Vestibulo-Motor Circuit Specificity. *Cell* 163, 301–312. <https://doi.org/10.1016/j.cell.2015.09.023>.
14. Cullen, K.E., and Taube, J.S. (2017). Our sense of direction: progress, controversies and challenges. *Nat. Neurosci.* 20, 1465–1473. <https://doi.org/10.1038/nn.4658>.
15. Berghuis, P., Rajnicek, A.M., Morozov, Y.M., Ross, R.A., Mulder, J., Urbán, G.M., Monory, K., Marsicano, G., Matteoli, M., Canti, A., et al. (2007). Hardwiring the brain: endocannabinoids shape neuronal connectivity. *Science* 316, 1212–1216. <https://doi.org/10.1126/science.1137406>.
16. Liu, Z., Hildebrand, D.G.C., Morgan, J.L., Jia, Y., Slimmon, N., and Bagnall, M.W. (2022). Organization of the gravity-sensing system in zebrafish. *Nat. Commun.* 13, 5060. <https://doi.org/10.1038/s41467-022-32824-w>.
17. Straka, H., Beraneck, M., Rohrger, M., Moore, L.E., Vidal, P.P., and Vibert, N. (2004). Second-order vestibular neurons form separate populations with different membrane and discharge properties. *J. Neurophysiol.* 92, 845–861. <https://doi.org/10.1152/jn.00107.2004>.
18. Yang, G.R., Murray, J.D., and Wang, X.J. (2016). A dendritic disinhibitory circuit mechanism for pathway-specific gating. *Nat. Commun.* 7, 12815. <https://doi.org/10.1038/ncomms12815>.
19. Wang, Y., Kakizaki, T., Sakagami, H., Saito, K., Ebihara, S., Kato, M., Hirabayashi, M., Saito, Y., Furuya, N., and Yanagawa, Y. (2009). Fluorescent labeling of both GABAergic and glycinergic neurons in vesicular GABA transporter (VGAT)-Venus transgenic mouse. *Neurosci.* 164, 1031–1043. <https://doi.org/10.1016/j.neuroscience.2009.09.010>.
20. Rusnak, F., and Mertz, P. (2000). Calcineurin: form and function. *Physiol. Rev.* 80, 1483–1521. <https://doi.org/10.1152/physrev.2000.80.4.1483>.
21. Zeng, H., Chattarji, S., Barbarosie, M., Rondi-Reig, L., Philpot, B.D., Miyakawa, T., Bear, M.F., and Tonegawa, S. (2001). Forebrain-specific calcineurin knockout selectively impairs bidirectional synaptic plasticity and working/episodic-like memory. *Cell* 107, 617–629. [https://doi.org/10.1016/s0092-8674\(01\)00585-2](https://doi.org/10.1016/s0092-8674(01)00585-2).
22. Malleret, G., Haditsch, U., Genoux, D., Jones, M.W., Bliss, T.V., Vanhoose, A.M., Weitlauf, C., Kandel, E.R., Winder, D.G., and Mansuy, I.M. (2001). Inducible and reversible enhancement of learning, memory, and long-term potentiation by genetic inhibition of calcineurin. *Cell* 104, 675–686. [https://doi.org/10.1016/s0092-8674\(01\)00264-1](https://doi.org/10.1016/s0092-8674(01)00264-1).
23. Wang, D.D., and Kriegstein, A.R. (2011). Blocking early GABA depolarization with bumetanide results in permanent alterations in cortical circuits and sensorimotor gating deficits. *Cereb. Cortex* 21, 574–587. <https://doi.org/10.1093/cercor/bhq124>.
24. Sagar, K.A., and Gruber, S.A. (2019). Interactions between recreational cannabis use and cognitive function: lessons from functional magnetic resonance imaging. *Ann. N. Y. Acad. Sci.* 1451, 42–70. <https://doi.org/10.1111/nyas.13990>.
25. Hensch, T.K. (2005). Critical period plasticity in local cortical circuits. *Nat. Rev. Neurosci.* 6, 877–888. <https://doi.org/10.1038/nrn1787>.
26. Lu, H.C., and Mackie, K. (2016). An Introduction to the eEndogenous cannabinoid system. *Biol. Psychiatry* 79, 516–525. <https://doi.org/10.1016/j.biopsych.2015.07.028>.
27. Chiu, C.Q., Barberis, A., and Higley, M.J. (2019). Preserving the balance: diverse forms of long-term GABAergic synaptic plasticity. *Nat. Rev. Neurosci.* 20, 272–281. <https://doi.org/10.1038/s41583-019-0141-5>.
28. Shi, J., Damjanoska, K.J., Zemaitaitis, B., Garcia, F., Carrasco, G., Sullivan, N.R., She, Y., Young, K.H., Battaglia, G., Van De Kar, L.D., et al. (2006). Alterations in 5-HT2A receptor signaling in male and female transgenic rats over-expressing either Gq or RGS-insensitive Gq protein. *Neuropharmacology* 51, 524–535. <https://doi.org/10.1016/j.neuropharm.2006.04.012>.
29. Gales, C., Kowalski-Chauvel, A., Dufour, M.N., Seva, C., Moroder, L., Pradayrol, L., Vaysse, N., Fourmy, D., and Silvente-Poirot, S. (2000). Mutation of Asn-391 within the conserved NPXXY motif of the cholecystokinin B receptor abolishes Gq protein activation without affecting its association with the receptor. *J. Biol. Chem.* 275, 17321–17327. <https://doi.org/10.1074/jbc.M909801199>.
30. Best, A.R., and Regehr, W.G. (2008). Serotonin evokes endocannabinoid release and retrogradely suppresses excitatory synapses. *J. Neurosci.* 28, 6508–6515. <https://doi.org/10.1523/JNEUROSCI.0678-08.2008>.
31. Bowers, M.E., and Ressler, K.J. (2015). Interaction between the cholecystokinin and endogenous cannabinoid systems in cued fear expression and extinction retention. *Neuropsychopharmacology* 40, 688–700. <https://doi.org/10.1038/npp.2014.225>.
32. Shanes, B.C., Winder, D.G., Patel, S., and Colbran, R.J. (2015). The initiation of synaptic 2-AG mobilization requires both an increased supply of diacylglycerol precursor and increased postsynaptic calcium. *Neuropharmacology* 91, 57–62. <https://doi.org/10.1016/j.neuropharm.2014.11.026>.
33. Chevaleyre, V., Heifets, B.D., Kaeser, P.S., Südhof, T.C., and Castillo, P.E. (2007). Endocannabinoid-mediated long-term plasticity requires cAMP/PKA signaling and RIM1alpha. *Neuron* 54, 801–812. <https://doi.org/10.1016/j.neuron.2007.05.020>.
34. Colmers, P.L.W., and Bains, J.S. (2018). Presynaptic mGluRs control the duration of endocannabinoid-mediated DSI. *J. Neurosci.* 38, 10444–10453. <https://doi.org/10.1523/JNEUROSCI.1097-18.2018>.
35. Huang, G.Z., and Woolley, C.S. (2012). Estradiol acutely suppresses inhibition in the hippocampus through a sex-specific endocannabinoid and mGluR-dependent mechanism. *Neuron* 74, 801–808.
36. Wilson, R.I., and Nicoll, R.A. (2002). Endocannabinoid signaling in the brain. *Science* 296, 678–682. <https://doi.org/10.1126/science.1063545>.
37. Heifets, B.D., and Castillo, P.E. (2009). Endocannabinoid signaling and long-term synaptic plasticity. *Annu. Rev. Physiol.* 71, 283–306. <https://doi.org/10.1146/annurev.physiol.010908.163149>.

38. Wallace, D.G., Hines, D.J., Pellis, S.M., and Whishaw, I.Q. (2002). Vestibular information is required for dead reckoning in the rat. *J. Neurosci.* 22, 10009–10017. <https://doi.org/10.1523/JNEUROSCI.22-22-10009.2002>.

39. Scheyer, A.F., Borsoi, M., Wager-Miller, J., Pelissier-Alicot, A.L., Murphy, M.N., Mackie, K., and Manzoni, O.J.J. (2020). Cannabinoid exposure via lactation in rats disrupts perinatal programming of the gamma-aminobutyric acid trajectory and select early-life Behaviors. *Biol. Psychiatry* 87, 666–677. <https://doi.org/10.1016/j.biopsych.2019.08.023>.

40. Huang, Z.J., Kirkwood, A., Pizzorusso, T., Porciatti, V., Morales, B., Bear, M.F., Maffei, L., and Tonegawa, S. (1999). BDNF regulates the maturation of inhibition and the critical period of plasticity in mouse visual cortex. *Cell* 98, 739–755. [https://doi.org/10.1016/s0092-8674\(00\)81509-3](https://doi.org/10.1016/s0092-8674(00)81509-3).

41. Berardi, N., Pizzorusso, T., and Maffei, L. (2000). Critical periods during sensory development. *Curr. Opin. Neurobiol.* 10, 138–145. [https://doi.org/10.1016/s0959-4388\(99\)00047-1](https://doi.org/10.1016/s0959-4388(99)00047-1).

42. Wang, D.D., and Kriegstein, A.R. (2008). GABA regulates excitatory synapse formation in the neocortex via NMDA receptor activation. *J. Neurosci.* 28, 5547–5558. <https://doi.org/10.1523/JNEUROSCI.5599-07.2008>.

43. Chancey, J.H., Adlaf, E.W., Sapp, M.C., Pugh, P.C., Wadicche, J.I., and Overstreet-Wadicche, L.S. (2013). GABA depolarization is required for experience-dependent synapse unsilencing in adult-born neurons. *J. Neurosci.* 33, 6614–6622. <https://doi.org/10.1523/JNEUROSCI.0781-13.2013>.

44. Sim-Selley, L.J. (2003). Regulation of cannabinoid CB1 receptors in the central nervous system by chronic cannabinoids. *Crit. Rev. Neurobiol.* 15, 91–119. <https://doi.org/10.1615/critrevneurobiol.v15.i2.10>.

45. Henderson-Redmond, A.N., Nealon, C.M., Davis, B.J., Yuill, M.B., Sepulveda, D.E., Blanton, H.L., Piscura, M.K., Zee, M.L., Haskins, C.P., Marcus, D.J., et al. (2020). c-Jun N terminal kinase signaling pathways mediate cannabinoid tolerance in an agonist-specific manner. *Neuropharmacology* 164, 107847. <https://doi.org/10.1016/j.neuropharm.2019.107847>.

46. Morgan, D.J., Davis, B.J., Kearn, C.S., Marcus, D., Cook, A.J., Wager-Miller, J., Straiker, A., Myoga, M.H., Karduck, J., Leishman, E., et al. (2014). Mutation of putative GRK phosphorylation sites in the cannabinoid receptor 1 (CB1R) confers resistance to cannabinoid tolerance and hyper-sensitivity to cannabinoids in mice. *J. Neurosci.* 34, 5152–5163. <https://doi.org/10.1523/JNEUROSCI.3445-12.2014>.

47. Burston, J.J., Wiley, J.L., Craig, A.A., Selley, D.E., and Sim-Selley, L.J. (2010). Regional enhancement of cannabinoid CB1 receptor desensitization in female adolescent rats following repeated Delta-tetrahydrocannabinol exposure. *Br. J. Pharmacol.* 161, 103–112. <https://doi.org/10.1111/j.1476-5381.2010.00870.x>.

48. Wilson, R.I., Kunos, G., and Nicoll, R.A. (2001). Presynaptic specificity of endocannabinoid signaling in the hippocampus. *Neuron* 31, 453–462. [https://doi.org/10.1016/s0896-6273\(01\)00372-5](https://doi.org/10.1016/s0896-6273(01)00372-5).

49. Malinvaud, D., Vassias, I., Reichenberger, I., Rössert, C., and Straka, H. (2010). Functional organization of vestibular commissural connections in frog. *J. Neurosci.* 30, 3310–3325. <https://doi.org/10.1523/JNEUROSCI.5318-09.2010>.

50. Grassi, S., Frondaroli, A., Dieni, C., Scarduzio, M., and Pettorossi, V.E. (2009). Long-term potentiation in the rat medial vestibular nuclei depends on locally synthesized 17beta-estradiol. *J. Neurosci.* 29, 10779–10783. <https://doi.org/10.1523/JNEUROSCI.1697-09.2009>.

51. Pettorossi, V.E., Dieni, C.V., Scarduzio, M., and Grassi, S. (2011). Long-term potentiation of synaptic response and intrinsic excitability in neurons of the rat medial vestibular nuclei. *Neuroscience* 187, 1–14. <https://doi.org/10.1016/j.neuroscience.2011.04.040>.

52. Straka, H., and Dieringer, N. (1996). Uncrossed disynaptic inhibition of second-order vestibular neurons and its interaction with monosynaptic excitation from vestibular nerve afferent fibers in the frog. *J. Neurophysiol.* 76, 3087–3101. <https://doi.org/10.1152/jn.1996.76.5.3087>.

53. McElvain, L.E., Bagnall, M.W., Sakatos, A., and du Lac, S. (2010). Bidirectional plasticity gated by hyperpolarization controls the gain of postsynaptic firing responses at central vestibular nerve synapses. *Neuron* 68, 763–775. <https://doi.org/10.1016/j.neuron.2010.09.025>.

54. Cullen, K.E. (2012). The vestibular system: multimodal integration and encoding of self-motion for motor control. *Trends Neurosci.* 35, 185–196. <https://doi.org/10.1016/j.tins.2011.12.001>.

55. Gittis, A.H., and du Lac, S. (2006). Intrinsic and synaptic plasticity in the vestibular system. *Curr. Opin. Neurobiol.* 16, 385–390. <https://doi.org/10.1016/j.conb.2006.06.012>.

56. O'Keefe, J., and Burgess, N. (1996). Geometric determinants of the place fields of hippocampal neurons. *Nature* 381, 425–428. <https://doi.org/10.1038/381425a0>.

57. Hafting, T., Fyhn, M., Molden, S., Moser, M.B., and Moser, E.I. (2005). Microstructure of a spatial map in the entorhinal cortex. *Nature* 436, 801–806. <https://doi.org/10.1038/nature03721>.

58. Cornwell, B.R., Johnson, L.L., Holroyd, T., Carver, F.W., and Grillon, C. (2008). Human hippocampal and parahippocampal theta during goal-directed spatial navigation predicts performance on a virtual Morris water maze. *J. Neurosci.* 28, 5983–5990. <https://doi.org/10.1523/JNEUROSCI.5001-07.2008>.

STAR★METHODS

KEY RESOURCES TABLE

REAGENT or RESOURCE	SOURCE	IDENTIFIER
Chemicals, peptides, and recombinant proteins		
WIN55 ((3R)-2,3-dihydro-5-methyl-3-(4-morpholinylmethyl)pyrrolo [1,2,3-de]-1,4-benzoxazin-6-yl)-1-naphthalenyl-methanone, monomethanesulfonate)	Tocris Bioscience 1038/10	
CNQX	Tocris Bioscience 0190/10	
D-AP5	Tocris Bioscience 0106/1	
FK506	Tocris Bioscience 3631	
BIC (bicuculline methiodide)	Tocris Bioscience 0131/10	
TTX	Sigma-Aldrich 554412	
AM251 (N-(Piperidin-1-yl)-5-(4-iodophenyl)-1-(2,4-dichlorophenyl)-4-methyl-1H-pyrazole-3-carboxamide)	Tocris Bioscience 1117/1	
SR141716A (N-(Piperidin-1-yl)-5-(4-chlorophenyl)-1-(2,4-dichlorophenyl)-4-methyl-1H-pyrazole-3-carboxamide hydrochloride)	Tocris Bioscience 0923/10	
BAPTA AM	Tocris Bioscience 2787/25	
7,8-dihydroxyflavone (7,8-dihydroxy-2-phenyl-4H-1-benzopyran-4-one)	Tocris Bioscience 3826/10	
MPEP (2-methyl-6-(phenylethynyl)pyridine hydrochloride)	Tocris Bioscience 1212/10	
K252a ((9S,10R,12R)-2,3,9,10,11,12-hexahydro-10-hydroxy-9-methyl-1-oxo-9,12-epoxy-1H-diindolo[1,2,3-fg:3',2',1'-kl]pyrrolo[3,4-i][1,6]benzodiazocine-10-carboxylic acid methyl ester)	Tocris Bioscience 1683/200U	
LY367385 ((S)-(+)- α -Amino-4-carboxy-2-methylbenzeneacetic acid), DHPG (RS)-3,5-dihydroxyphenylglycine	Tocris Bioscience 1237/10	
JZL184 (4-[Bis(1,3-benzodioxol-5-yl)hydroxymethyl]-1-piperidinecarboxylic acid 4-nitrophenyl ester)	Tocris Bioscience 3836/10	
Orlistat (N-formyl-L-leucine (1S)-1-[(2S,3S)-3-hexyl-4-oxo-2-oxetanyl]methyl]dodecyl ester)	Tocris Bioscience 3540/10	
CCK (cholecystokinin)	Tocris Bioscience 1166/1	
CI988	Tocris Bioscience 2607/10	
U73122 (1-[6-[(17 β)-3-Methoxyestra-1,3,5(10)-trien-17-yl]amino]hexyl)-1H-pyrrole-2,5-dione)	Tocris Bioscience 1268/10	
KT5720 ((9R,10S,12S)-2,3,9,10,11,12-Hexahydro-10-hydroxy-9-methyl-1-oxo-9,12-epoxy-1H-diindolo[1,2,3-fg:3',2',1'-kl]pyrrolo[3,4-i][1,6]benzodiazocine-10-carboxylic acid, hexyl ester)	Tocris Bioscience 1288/100U	

(Continued on next page)

Continued

REAGENT or RESOURCE	SOURCE	IDENTIFIER
MDL11939 (α -Phenyl-1-(2-phenylethyl)-4-piperidinemethanol)	Tocris Bioscience 0870/10	
α -m-5HT (α -Methyl-5-hydroxytryptamine maleate)	Tocris Bioscience	

EXPERIMENTAL MODEL AND STUDY PARTICIPANT DETAILS**Animals**

Sprague-Dawley rats (Charles River Lab), C57Bl6/J mice (Jackson Laboratory), vesicular GABA transporter (VGAT)-Venus transgenic mice¹⁹ (a gift from Professor Y Yanagawa, Gunma University Graduate School of Medicine), and CB1R knockout ($Cnr1^{-/-}$) mice (Shanghai Model Organisms Center Incorporated) were used. For experiments conducted on adults, only male rats were used. Early postnatal animals were randomly picked for electrophysiological and behavioral experiments as the sex of rodents prior to weaning is not explicit. Procedures were approved either by The University of Hong Kong Committee on the Use of Live Animals in Teaching and Research or by Beihang University Ethics Review Board.

METHOD DETAILS**Surgery implantation of Elvax slice**

200 μ L of 10 mM CB1 receptor agonist WIN55 and/or 10 mM CB1 receptor antagonist AM251 solution in dimethyl sulfoxide (DMSO, 4%, Sigma) were mixed and snap frozen with a 10% (w/v) Elvax solution in dichloromethane as described previously. Solidified slices were kept at -20 C to allow evaporation of dichloromethane. Slices cut to final dimensions (1 mm \times 1 mm, 200 μ m thickness) prior to implantation to the 4th ventricle via the foramen magnum.

Dead reckoning behavioral test

Dead reckoning test for spatial cognition was conducted on P60 rats implanted with drug-loaded Elvax slices at P1, P8 or P12, and sham operated rats. Rats were fasted for 12 h prior to test sessions. Only one food pellet (1 g, Supreme Mini-Treats, Bio-Serv) was provided during each test trial. Rats foraged for the food pellet placed randomly around the middle of the circular arena before returning to their home cage in 1 of the 8 possible locations around the arena. Stationary visual cues were provided during the training sessions and light probe tests. In the dark probe test, the lights were switched off and the arena was surrounded completely by a ceiling-to-floor black curtain. The new home location test was conducted in light with the home base moved to the hole diametrically opposite to its original home base. Eight trials were done in each of the light or dark probe tests and 4 in the new location test spread over 3 consecutive days (Figure S10). Heading angle, time in the quadrant with food, errors the rats made in return path, and the training time needed before rats learnt the task were measured from recorded video footage.

Patch clamp recording

Borosilicate glass pipettes (4–6 M Ω) filled with internal solution for voltage clamp containing (in mM): 140 KCl, 2 MgCl₂, 2 Na₂ATP, 1 ethylene glycol-bis (b-aminoethyl ether)-N,N,N',N'-tetra-acetic acid (EGTA), and 10 N-2-hydroxyethylpiperazine-N'-2-ethanesulphonic acid (HEPES) (adjusted to pH 7.3, 285–295 mOsm) were used. KCl-based internal solution was used to record evoked GABAergic postsynaptic currents (ePSC_{GABA}). For current-clamp recordings, electrodes were filled with an internal solution containing the following (in mM): 134 K-gluconate, 6 KCl, 10 HEPES, 4 NaCl, 7 K₂-phosphocreatine, 0.3 NaGTP, and 4 Mg-ATP (pH 7.3 adjusted with KOH). No series resistance compensation was applied but the cell was discarded if the access resistance changed significantly (>25%) during the course of recording. Cell recording was discarded if the leaking current was >100 pA.

QUANTIFICATION AND STATISTICAL ANALYSIS

The statistical analyses were performed using GraphPad Prism 9 software. All statistical details of the experiments can be found in the figures and figure legends. All data are presented as mean \pm SEM. One-way ANOVA followed by Bonferroni's correction for multiple comparison was used to compare the average time for accomplishing positive responses in negative geotaxis and air righting tests, as well as performance indexes in the dead reckoning test. Differences with $p < 0.05$ were considered statistically significant.